

# High-frequency genetic reversion mediated by a DNA duplication: The mouse pink-eyed unstable mutation

(mitotic recombination/homologous recombination/illegitimate recombination)

YOICHI GONDO\*, JOHN M. GARDNER, YOSHIMICHI NAKATSU, DONNA DURHAM-PIERRE, SUSAN A. DEVEAU†, CYNTHIA KUPER, AND MURRAY H. BRILLIANT‡

The Institute for Cancer Research, Fox Chase Cancer Center, 7701 Burlholme Avenue, Philadelphia, PA 19111

Communicated by Mary F. Lyon, September 28, 1992 (received for review July 8, 1992)

**ABSTRACT** The mouse pink-eyed unstable ( $p^{un}$ ) mutation, affecting coat color, exhibits one of the highest reported reversion frequencies of any mammalian mutation and is associated with a duplication of genomic DNA at the  $p$  locus. In this study, genomic clones containing the boundaries of the  $p^{un}$  duplication were isolated and characterized. The structure of these sequences and their wild-type and revertant counterparts were analyzed by restriction mapping, PCR product analysis, DNA sequence analysis, and pulsed-field gel electrophoresis. DNA from  $p^{un}$  was distinguished from wild-type and revertant DNA by a head-to-tail tandem duplication of  $\approx 70$  kilobases. No differences were detected between revertant and wild-type DNAs. Thus, the reversion in phenotype of  $p^{un}$  mice is coupled with the loss of one copy of an  $\approx 70$ -kilobase duplicated segment. Testable models are presented to account for  $p^{un}$  reversion.

The pink-eyed unstable mutation,  $p^{un}$  (1), arose spontaneously in the inbred strain C57BL/6J and is one of at least 13 mutant (recessive) alleles of the pink-eyed dilution locus,  $p$ , on mouse chromosome 7. The phenotypes of homozygous mutants of  $p$  range from a minor reduction in coat color to a dramatic reduction of both coat and eye color. The gene responsible for the pigmentation phenotype has been identified and cloned (2). However, in addition to pigmentation, several mutant  $p$  alleles are associated with other phenotypes, including neurological disorders ( $p^{6H}$ ,  $p^{25H}$ ,  $p^{bs}$ ,  $p^{cp}$ ), cleft palate ( $p^{cp}$ ), male sterility ( $p^{6H}$ ,  $p^{25H}$ ,  $p^{bs}$ ), prenatal lethality ( $p^{81H}$ ,  $p^{82H}$ ,  $p^{87H}$ ), and genetic instability ( $p^{un}$ ) (3–6). The genetic instability of the  $p^{un}$  mutation is manifest as one of the highest spontaneous reversion frequencies reported for a mammalian mutation. At least 1.8% of the offspring of  $p^{un}/p^{un}$  mice are mosaic revertants—i.e., light colored with black streaks or patches (7). Reversion in  $p^{un}/p^{un}$  mice is primarily detected as a somatic event but can occur in germ cells or their precursors and be transmitted through the germ line. Revertant lines are indistinguishable from C57BL/6J wild-type mice and the revertant phenotype is stable over many generations (8).

In a previous study, we used the genome scanning method to identify a duplication in  $p^{un}$  DNA (8). When used as a hybridization probe, a clone from inside the duplication, 28RN, revealed a  $p^{un}$ -specific 15-kilobase (kb) *Sst* I fragment (a putative boundary of the  $p^{un}$  duplication). In the present study, data are presented demonstrating that the  $p^{un}$  duplication is a tandem head-to-tail duplication of  $\approx 70$  kb and testable models are presented to account for genetic reversion.<sup>§</sup>

## MATERIALS AND METHODS

**Mice, Genomic DNA Isolation.** All mice used in this study were obtained from or produced at The Jackson Laboratory

or The Institute for Cancer Research, Fox Chase Cancer Center (Philadelphia). Revertant alleles  $p^{un+1J}$ ,  $p^{un+2J}$ ,  $p^{un+3J}$ ,  $p^{un+5J}$ , and  $p^{un+6J}$  were derived from independent revertant mice as described (8). All  $p$  alleles used in this study, except for the  $p^{6H}$  allele, are coisogenic on the inbred strain C57BL6/JEi. The  $p^{6H}$  allele was originally generated in the course of x-ray mutagenesis experiments at the MRC Radiobiology Unit, Harwell (9). Genomic DNAs for standard Southern analysis were isolated as reported (8).

**$\lambda$  Library Construction, Restriction Mapping, Subcloning.** The clone  $\lambda$ U500 was isolated from a size-selected genomic library generated by ligating  $\approx 15$ -kb *Sst* I-digested genomic  $p^{un}/p^{un}$  fragments (purified on a sucrose gradient) into *Sst* I-digested Lambda DASH (Stratagene). The hybridization probe used to select  $\lambda$ U500 was the 28RN fragment (8).

An 850-base-pair (bp) *Hind*III/*Sst* I fragment (HS fragment) was isolated from the  $\lambda$ U500 clone and subcloned into a pUC9 plasmid vector, pHS. The HS fragment was used as a hybridization probe to select three other  $\lambda$  clones (each representing different genomic regions in  $p^{un}$  DNA)— $\lambda$ U300,  $\lambda$ U510, and  $\lambda$ U700. These phage were isolated from a second library generated by ligating *Sau*3A partially digested genomic DNA from a  $p^{un}/p^{un}$  mouse into *Bam*HI-digested Lambda DASH (Stratagene). Other phage were selected from this same library by chromosomal walking, including  $\lambda$ U480, containing sequences entirely within the  $p^{un}$  duplication. Plaque lifts were as published (10).

A 1.4-kb *Eco*RI fragment, 700R, was isolated from a region of  $\lambda$ U700 that was outside the  $p^{un}$  DNA duplication and was subcloned into a pUC13 plasmid vector, p700R. A 1.7-kb *Eco*RI/*Hind*III fragment, 300L, was isolated from a region of  $\lambda$ U300 that was outside the  $p^{un}$  DNA duplication (purified from subclone p21Eb, a pUC13-based plasmid containing a 4.8-kb *Eco*RI fragment). A 1.8-kb *Bam*HI/*Xba* I fragment, BX1.8, originating from  $\lambda$ U480 was used as a hybridization probe in some experiments. Under the hybridization and washing conditions used, fragments HS, BX1.8, 700R, and 300L behaved as unique sequence DNA.

**Gel Electrophoresis, Probe Preparation, Southern Hybridization.** Standard agarose gel electrophoresis, Southern blotting to GeneScreenPlus membranes (DuPont/NEN) or to Hybond-N+ (Amersham), and hybridization were as described (8). Probes were generated by using the Multiprime kit (Amersham) or the Prime-It kit (Stratagene) to a specific activity of  $1-3 \times 10^9$  cpm/ $\mu$ g.

**Pulsed-Field Gel Electrophoresis (PFGE).** DNA from mouse spleen cells was prepared and digested in agarose plugs (11).

Abbreviation: PFGE, pulsed-field gel electrophoresis.

\*Present address: Department of DNA Biology, School of Medicine, Tokai University, Bohseidai, Isehara, Kanagawa 259-11, Japan.

†Present address: The Jackson Laboratory, Bar Harbor, ME 04609.

‡To whom reprint requests should be addressed.

§The sequences reported in this paper have been deposited in the GenBank data base (accession nos. L07479, L07480, and L07481).

The publication costs of this article were defrayed in part by page charge payment. This article must therefore be hereby marked "advertisement" in accordance with 18 U.S.C. §1734 solely to indicate this fact.

Table 1. Oligonucleotide primers used

Primer	Sequence	Origin*	Location/orientation†
MHB7	5'-CTTATGAAGCAAGAATCAAC-3'	$\lambda$ U300, $\lambda$ U510	+188 → +169, Opp.
MHB8	5'-TTTTGATAGTCTGAAAAGAGC-3'	$\lambda$ U700, $\lambda$ U500, $\lambda$ U510	-215 → -196, Same
MHB9	5'-AGGATTCTGCTATCAGCCTT-3'	$\lambda$ U300	-256 → -237, Same
MHB10	5'-AAGTCCAATTAGGACAGATT-3'	$\lambda$ U700	+373 → +354, Opp.
MHB13‡	5'-CACTATGCCTGCTTGGATGCTGC-3'	$\lambda$ U300	-203 → -179, Same
MHB19‡	5'-CCAGCCAAACTGCCATTC-3'	$\lambda$ U700	+148 → +131, Opp.

\*Determined from partial sequence of the indicated  $\lambda$  clones or their derivatives.

†Numbering relative to the boundary TGG trinucleotide, where T is +1. Same, same strand; Opp., opposite strand.

‡Used as sequencing primer only.

Electrophoresis was performed with a model 2604 Waltzer II rotating stage apparatus (Tribotics, Oxford, U.K.) in 1% agarose gels [1:1 composites of GTG and Fast Lane agarose (FMC)] in 20 mM Tris acetate/1 mM EDTA at 16°C, using a 45-sec switch time. Molecular weight estimations were based on a  $\lambda$  phage DNA oligomer ladder and *Saccharomyces cerevisiae* chromosomal DNA (Bio-Rad).

**PCR, Oligonucleotide Primers, Cloning of PCR Products, and Sequence Determination.** DNA from wild-type,  $p^{un}/p^{un}$ , and revertants  $p^{un+1J}/p^{un+1J}$ ,  $p^{un+2J}/p^{un+2J}$ , and  $p^{un+3J}/p^{un+3J}$  was amplified from genomic DNA using a programmable thermal controller (MJ Research, Watertown, MA): 94°C for 2 min; 94°C for 1 min; 52°C for 30 sec; 72°C for 1 min 30 sec; repeat steps 2–4 39 times; 72°C for 5 min; hold at 15°C (end). The following primer pairs (obtained from The DNA Synthesis Facility, Fox Chase Cancer Center) were used: MHB9 and MHB7, MHB8 and MHB7, and MHB8 and MHB10. Table 1 summarizes the primer sequences, origin, location, and orientation relative to the  $p^{un}$  duplication junction.

The PCRs were carried out in 50  $\mu$ l, under conditions recommended by the supplier (Perkin-Elmer/Cetus kit), with the following modifications: 30  $\mu$ l (500 ng) of genomic DNA, 2.5  $\mu$ l of each primer pair (at 20  $\mu$ M, except MHB9 at 5  $\mu$ M), 0.5  $\mu$ l of Perfect Match (Stratagene), 0.5  $\mu$ l of 100 mM MgCl<sub>2</sub>. Aliquots of the PCRs were resolved in an agarose gel composed of 1% agarose (BRL)/1% NuSieve agarose (FMC) and blotted for Southern analysis (8). Other aliquots were used to obtain gel-purified (12) PCR products using DE81 paper (Whatman) for subcloning into plasmids via the TA Cloning kit (Invitrogen). The sequence of the cloned PCR product DNA was determined for two or three independent clones each from wild-type,  $p^{un}/p^{un}$ , and revertants  $p^{un+1J}/p^{un+1J}$ ,  $p^{un+2J}/p^{un+2J}$ , and  $p^{un+3J}/p^{un+3J}$ . The sequencing primers used were MHB8, MHB7, MHB13, and MHB19 (Table 1), and 17-mer pUC/M13 primers (Promega). Sequencing was performed by the dideoxynucleotide chain-termination method (13), as modified by the Sequenase kit (United States Biochemical).

## RESULTS

**Cloning the  $p^{un}$  Duplication Boundaries.** To examine the molecular structure of the  $p^{un}$  duplication, we isolated a 15-kb  $p^{un}$ -specific *Sst* I fragment in  $\lambda$  phage ( $\lambda$ U500) previously shown to contain a boundary of the  $p^{un}$  duplication (8). In the previous study, the 15-kb  $p^{un}$ -specific *Sst* I fragment was shown to contain sequences in common with a 25-kb *Sst* I fragment found in wild-type,  $p^{un}$ , and revertant mice. Comparative restriction analysis of these two fragments narrowed the putative boundary of the  $p^{un}$  duplication to within an 850-bp *Hind*III/*Sst* I (HS) fragment of  $\lambda$ U500. A restriction map of the 15-kb  $\lambda$ U500 clone (showing the positions of 28RN, the original probe sequence, and the HS fragment) and its relationship to the 25-kb *Sst* I fragment is presented in Fig. 1.

The HS and 28RN fragments were used in parallel as hybridization probes to *Sst* I-digested genomic DNAs from wild-type,  $p^{un}$ , and revertant mice (Fig. 1). Predictably, the HS probe hybridized to its 15-kb *Sst* I fragment of origin in

$p^{un}$  DNA. The HS probe also hybridized to the same 25-kb *Sst* I fragment originally recognized by the 28RN probe in wild-type,  $p^{un}$ , and revertant DNA, indicating that the HS fragment still contains a significant portion of sequences common to both the 15- and 25-kb *Sst* I fragments. In addition, the HS fragment hybridized to a 1.8-kb *Sst* I fragment in all three genotypes.

Because the 15-kb *Sst* I fragment (containing the HS fragment) shares sequences with both the 25- and 1.8-kb *Sst* I fragments, it defines a unique junction of the  $p^{un}$  duplication (an apparent internal boundary of the duplication). The nonunique (apparent external) boundaries of the duplication are thus defined by the 25- and 1.8-kb *Sst* I fragments that are invariant in all three genotypes. To determine exactly how these fragments relate to the structure of the  $p^{un}$  duplication, we set out to clone and characterize sequences related to each of them.

**Structure of the  $p^{un}$  Duplication Boundaries.** We screened a total genomic library (prepared from *Sau*3A partially digested  $p^{un}$  DNA; see *Materials and Methods*) with the HS probe and isolated three classes of  $\lambda$  phage, representing the boundaries of the  $p^{un}$  duplication. Among the clones studied in detail were  $\lambda$ U300 (containing the 1.8-kb *Sst* I fragment),  $\lambda$ U510 (containing sequences from the 15-kb *Sst* I fragment), and  $\lambda$ U700 (containing sequences from the 25-kb *Sst* I fragment). Because all of these fragments were originally derived from  $p^{un}$  DNA, their characterization alone could not tell us about the genomic structure and sequence of homologous regions in

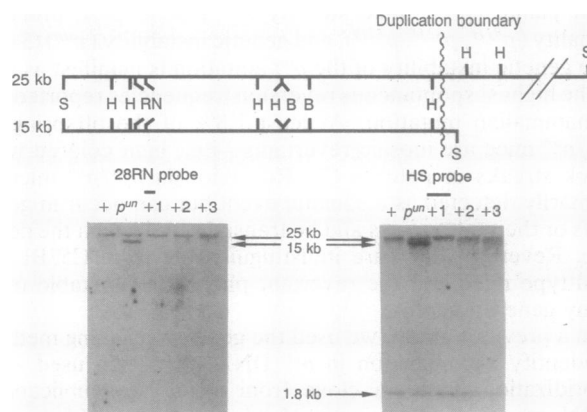


FIG. 1. (Upper) Restriction map of mutant-specific 15-kb *Sst* I insert of  $\lambda$ U500 and its relationship to the common 25-kb *Sst* I genomic fragment. Common *Sst* I (S), *Hind*III (H), and *Bam*HI (B) sites are indicated between the sequences. (There are other *Hind*III and *Bam*HI sites in the nonidentical part of the 25-kb *Sst* I fragment; data not shown.) Only the *Rsa* I (R) and *Nde* I (N) sites defining the 28RN fragment are shown. The duplication boundary (wavy line) where the 15-kb *Sst* I fragment diverges from the 25-kb *Sst* I fragment is within the 850-bp HS fragment. Locations of fragments (28RN and HS) used as probes in Southern analysis are indicated below the restriction map. (Lower) Southern blot of wild-type (+),  $p^{un}$ , and revertant DNAs ( $p^{un+1J}$ , +1;  $p^{un+2J}$ , +2;  $p^{un+3J}$ , +3) cut with *Sst* I and hybridized with the 28RN probe (Left) or HS probe (Right).

wild-type and revertant DNAs. However, the partial sequence analysis of these phage and their derivative subclones enabled us to synthesize oligonucleotide primers to analyze corresponding sequences in  $p^{un}$ , wild-type, and revertant DNAs using the PCR. The results of PCR analysis are shown in Fig. 2 and confirm that  $p^{un}$  DNA contains a junction of sequences not found in wild-type or revertant DNA (Fig. 2B and C, lanes 1 and 2). The orientation of the PCR primers (MHB8 and MHB7) that exclusively amplify  $p^{un}$  DNA indicates a head-to-tail orientation of the  $p^{un}$  duplication. To confirm this arrangement at the nucleotide level, we sequenced two or three independent cloned PCR products from wild-type,  $p^{un}/p^{un}$ , and revertants  $p^{un+1J}/p^{un+1J}$ ,  $p^{un+2J}/p^{un+2J}$ , and  $p^{un+3J}/p^{un+3J}$ . No sequence differences were found among any of the three independent revertant strains and wild type. The nucleotide sequences at the duplication junctions demonstrate that a head-to-tail tandem duplication has occurred in  $p^{un}$  DNA (Fig. 3). The boundaries of the duplication reside within a 3-nucleotide sequence, TGG, common to all boundary regions. We also noted a similarity of the sequences at the  $p^{un}$  duplication junction with the simian virus 40 and polyoma enhancer core sequences (14) and the more general consensus sequences of known sites of illegitimate recombination and DNA gyrase sites (15).

**Size of  $p^{un}$  Duplication.** To determine the size of the  $p^{un}$  duplication, genomic DNAs from  $p^{un}$ , wild-type, and revertant mice were digested with *Ksp* I and separated by PFGE. Southern blots of these DNAs were hybridized with probes 300L and 700R, unique sequence fragments from  $\lambda$ U300 and  $\lambda$ U700, respectively. Both probe sequences are outside the region duplicated in  $p^{un}$  DNA and neither probe hybridized to the genomic DNA of the radiation-induced  $p^{6H}$  mutation. A 610-kb *Ksp* I fragment was detected in wild-type and rever-

tant DNA with either probe, whereas a 680-kb *Ksp* I fragment was detected in  $p^{un}$  DNA using either probe (Fig. 4A). The same size difference between wild-type and  $p^{un}$  fragments was observed in *Nae* I digests (Fig. 4B). We derive four conclusions from these results: (i) there are no *Ksp* I or *Nae* I sites within the segment of DNA duplicated in  $p^{un}$  DNA; (ii) the unit length of the segment of DNA duplicated in  $p^{un}$  DNA is  $\approx 70$  kb, a result also confirmed by the analysis of contiguous  $\lambda$  phage and cosmid clones (data not shown); (iii) one copy of the segment of DNA duplicated in  $p^{un}$  DNA disappears upon reversion; and (iv) phenotypic mosaicism is the result of genotypic mosaicism.

## DISCUSSION

**Structure and Orientation of the  $p^{un}$  Duplication.** We have found that the basis for the spontaneous mutation  $p^{un}$  is a head-to-tail duplication of  $\approx 70$  kb. A comparison of the sequences at the junctions of the segment of DNA duplicated in  $p^{un}$  with corresponding sequences in wild-type mice indicated that the duplication was apparently exact; there were no sequence anomalies at the duplication boundaries in  $p^{un}$  DNA. PFGE demonstrates that the reversion of  $p^{un}$  is accompanied by the loss of one of the duplicated  $\approx 70$ -kb units. From sequence analysis of the junctions and PFGE data, we have deduced the structure of the duplication in relationship to the cloned sequences used in this study (Fig. 5A).

The sequences at the  $p^{un}$  duplication junctions (Fig. 3) may have served to promote the formation of the  $p^{un}$  duplication. These junction sequences resemble viral enhancers (14) and match 8 of 9 nucleotides of the consensus sequence of DNA gyrase sites and sites of illegitimate recombination (15). Although random sequence matches of this type are expected

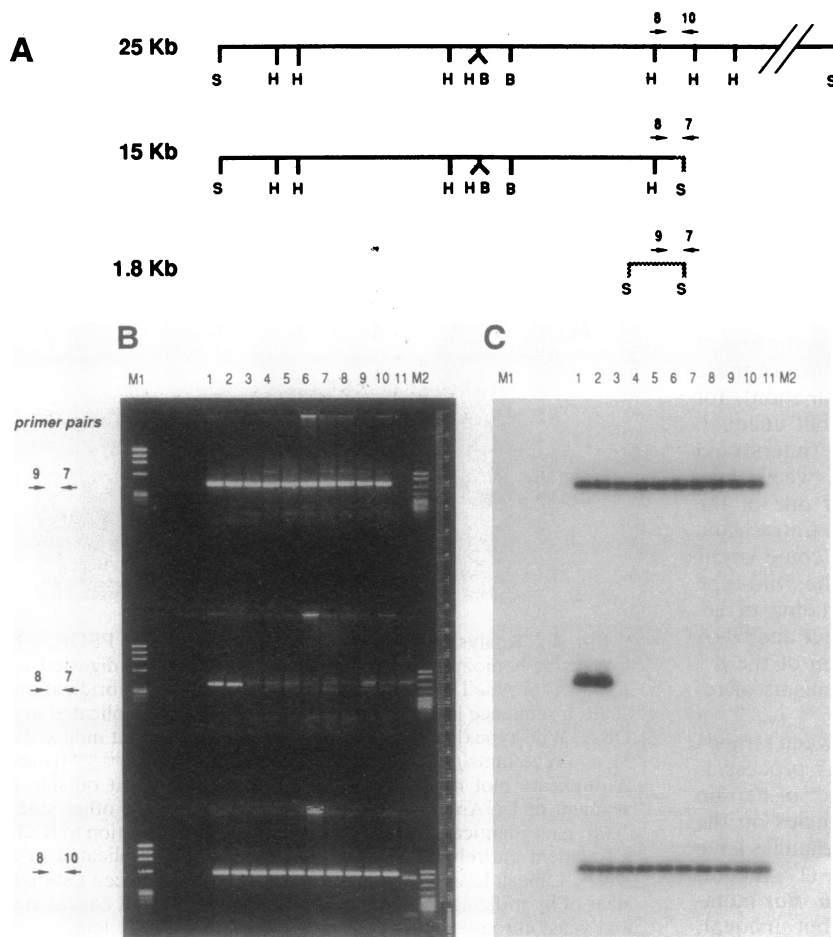


FIG. 2. PCR analysis of genomic DNA. (A) Location of PCR primers. Primers, deduced from the partial sequence of the HS fragment,  $\lambda$ U300,  $\lambda$ U500,  $\lambda$ U510, and  $\lambda$ U700, were used to synthesize corresponding genomic DNA fragments from  $p^{un}$ , wild-type, and revertant mice using PCR as described. (B) Ethidium bromide stain of PCR products. Top row, primer pairs MHB9 and MHB7 corresponding to sequences from  $\lambda$ U300; middle row, MHB8 and MHB7 corresponding to sequences from  $\lambda$ U500 and  $\lambda$ U510; bottom row, MHB8 and MHB10 corresponding to sequences from  $\lambda$ U700. Genomic DNAs from an individual male mouse (odd-numbered lanes) or female mouse (even-numbered lanes) homozygous for the indicated alleles were used in the PCRs. Lanes: 1 and 2,  $p^{un}$ ; 3 and 4, wild type; 5 and 6,  $p^{un+1J}$ ; 7 and 8,  $p^{un+2J}$ ; 9 and 10,  $p^{un+3J}$ ; 11,  $p^{6H}$ . Lane M1,  $\phi$ X174 replicative form DNA/*Hae* III markers; lane M2, pBR322 DNA/*Msp* I markers. (C) Southern blot analysis of same agarose gel shown in B hybridized to the HS probe (see Fig. 1), indicating the specific PCR products of B.

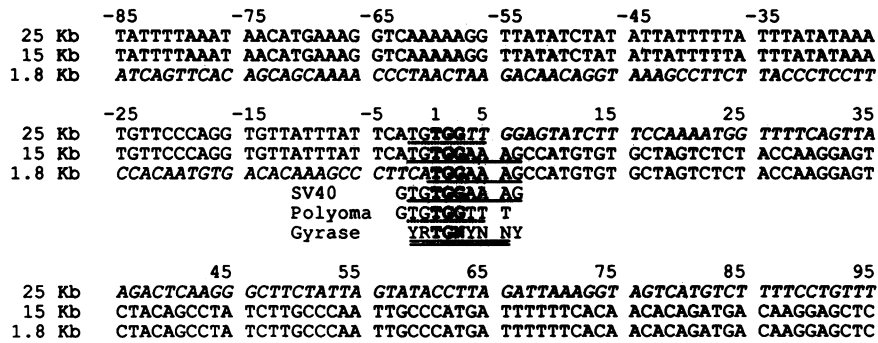


FIG. 3. Sequence overlap of the 15-kb *Sst* I ( $p^{m/m}$ -specific) fragment with the 25- and 1.8-kb *Sst* I fragments. A portion of the sequences determined from cloned PCR products is shown. DNA sequence derived from wild-type mice was identical to that from independent revertants  $p^{m/+1J}/p^{m/+1J}$ ,  $p^{m/+2J}/p^{m/+2J}$ , and  $p^{m/+3J}/p^{m/+3J}$ . PCR primer sequences (not shown) were specific for sequences within (or just outside of) the *Sst* I fragments, indicated on the left of each sequence (see Fig. 2 and *Materials and Methods*). Sequence identity between strands is indicated by normal type; sequence divergence between strands is indicated by italics. All sequences contain a common TGG (boldface type; nucleotides 1–3), 1 nucleotide of which is the point of divergence. The *Sst* I site common to both the 15- and 1.8-kb *Sst* I fragments lies at nucleotides 90–95. Nucleotide identity with the simian virus 40 enhancer (GTGTGGAAAG) is indicated by solid underline; nucleotide identity with the polyoma enhancer (GTGTGGTTT) is indicated by dotted underline (14). Sequences conforming to consensus gyrase sites and sites of illegitimate recombination (YRTGNYNY; where Y is pyrimidine, R is purine, and N is any nucleotide) are double underlined (15).

on the order of every  $10^4$ – $10^5$  nucleotides, it is also possible that the sequences at these sites may have played a role in generation of the  $p^{m/m}$  duplication.

**Reversion of the  $p^{m/m}$  Mutation.** Because mosaic revertant mice are also mosaic in DNA sequence, reversion must be a somatic (mitotic) event. We have found that reversion of the  $p^{m/m}$  phenotype is coupled with disappearance of the  $p^{m/m}$  duplication. No differences have been detected so far between the DNA of revertant mice and wild-type mice (although we have not exhaustively characterized the entire  $\approx 70$ -kb region in revertant mice). In particular, PFGE demonstrated the loss of DNA duplication (Fig. 4) and the DNA sequence at the duplication junctions of three independent revertants was found to be identical with that of wild-type DNA (Fig. 3). Moreover, we (2) have recently found that the  $p$  locus cDNA (with exons inside and outside of both ends of the  $p^{m/m}$  duplication unit) reveals the exact same Southern blot pattern in wild-type and revertant mice demonstrating that the colinearity and overall structure of this region is maintained—i.e., there are no gross sequence differences between wild-type and revertant DNA throughout the entire  $p$  locus. This apparent exact loss of the duplication unit in revertant mice strongly suggests an involvement of homologous recombination in the reversion process.

There are molecular processes that can result in the loss of sequences repeated in tandem. Two of the simplest of these processes (both involving homologous recombination), for which precedence exists, are (i) homologous, but unequal, crossing-over between the duplicated copies (interstrand recombination between sister chromatids or between chromosomal homologues), and (ii) looping-out of one of the duplicated copies within a single DNA strand (intrastrand recombination). In either case, recombination could occur anywhere within the  $\approx 70$ -kb unit to restore the wild-type sequence arrangement, consistent with our finding of sequence identity between DNA from wild-type mice and DNA from several independent revertants. A diagram of the  $p^{m/m}$  duplication showing these two potential mechanisms of reversion is shown in Fig. 5.

Homologous, but unequal, crossing-over between strands may underlie the cause of  $p^{m/m}$  reversion. This process is thought to mediate changes in the copy number of certain DNA sequences repeated in tandem at frequencies on the order of the  $p^{m/m}$  reversion frequency (16). These changes have been observed for both meiotic (18) and mitotic (17) recombination and include reversion of the *Drosophila Bar* mutation (19). A predicted product of homologous, but unequal,

crossing-over is a triplication of the unit (Fig. 5), as represented by the *double Bar* mutant allele of the *Drosophila Bar* locus (16, 19). In theory, this triplication should exist in equivalent amounts with the revertant (single unit) in mosaic mice. However, we did not detect a triplication-sized band in the single mosaic mouse analyzed (Fig. 4A). The predicted triplication may be inherently more unstable or confer a growth disadvantage. Consistent with the last hypothesis is our finding that  $p^{m/m}/p^{m/m}$  melanocytes grow significantly slower *in vitro* than melanocytes homozygous for the wild-type allele or melanocytes homozygous for other mutant alleles (data not shown). A second mechanism of reversion is looping-out. Looping-out produces a circular DNA product and is thought to occur somatically in immunoglobulin class switching (20) and may also occur somatically in the brain (21).

Melvold (22) has reported that reversion of  $p^{m/m}$  is impaired when recombination around the  $p$  locus is inhibited by a translocation, although these data may not be statistically significant. If true, this finding suggests that neither looping-out nor crossing-over between sister chromatids is the major mechanism underlying  $p^{m/m}$  reversion and implies that  $p^{m/m}$  reversion is most likely mediated by recombination between

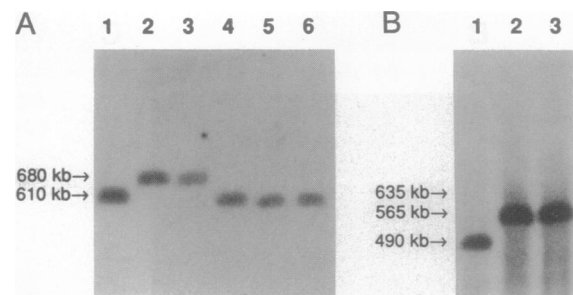


FIG. 4. Analysis of pink-eyed dilution locus using PFGE. DNA from mice homozygous for the indicated alleles was digested with *Ksp* I (A) or *Nae* I (B) and separated by PFGE. (A) Hybridization to 700R, a sequence just outside the segment of DNA duplicated in  $p^{m/m}$  DNA. Wild-type (lane 1);  $p^{m/m}$  (lane 2); mosaic revertant mouse (lane 3); and revertants  $p^{m/+1J}$  (lane 4),  $p^{m/+5J}$  (lane 5), and  $p^{m/+6J}$  (lane 6). A duplicate blot hybridized to 300R, a sequence just outside the segment of DNA duplicated in  $p^{m/m}$  DNA, but on the other side of 700R, gave identical results (not shown). (B) Hybridization to BX1.8, a fragment entirely within the segment of DNA duplicated in  $p^{m/m}$  DNA. Lanes: 1, wild-type; 2 and 3, two  $p^{m/m}/p^{m/m}$  mice. Estimated sizes of hybridizing fragments (based on migration of  $\lambda$  concatemers and yeast chromosomal markers) are indicated on the left.

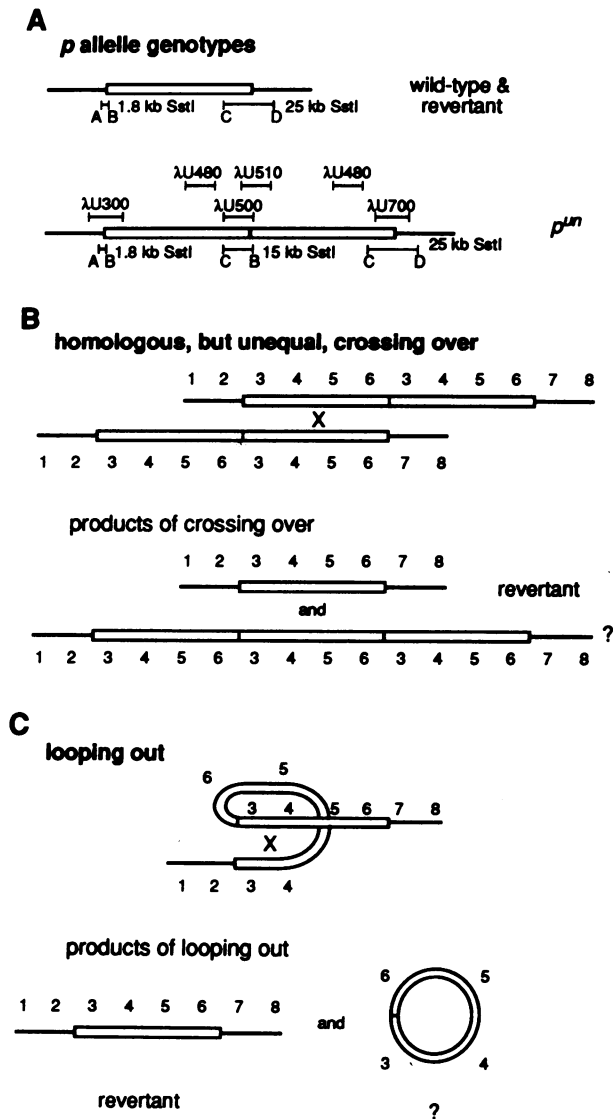


FIG. 5. Tandem head-to-tail duplication of  $p^{un}$  mutation and two models of its reversion. The unit of DNA that is duplicated in  $p^{un}$  DNA is shown as an open box. (A) Schematic representation of  $p$  allele genotypes with positions of *Sst* I fragments revealed by the HS probe. Individual *Sst* I sites of each fragment are lettered; homologous *Sst* I sites share the same letter. Relative positions of key  $\lambda$  phage clones are indicated. Other clones (not shown) establish a 70- to 75-kb contiguous sequence through the boxed region. Note that  $\lambda$ U480 is represented twice, as it contains sequences entirely within the  $p^{un}$  duplication. (B) Homologous, but unequal, crossing-over can occur between the duplicated units as has been observed in other systems (16, 17). Note that the order of linear information in the wild-type DNA sequence (represented by the sequence of numbers above or below the DNA lines) is disrupted by the  $p^{un}$  duplication. Products of homologous but unequal crossing-over are also shown:  $p^{un}$  revertant, with only one copy of the unit (identical in sequence order to wild type), and a predicted triplication of the unit. (C) Looping-out (intrastrand recombination), an alternative mechanism that can also result in loss of duplication. Products of looping-out are also shown:  $p^{un}$  revertant, with only one copy of the unit (identical in sequence order to wild type), and a predicted circle of the unit.

chromosomal homologues. However, more data are required to fully understand the reversion mechanism. Experiments to sort out these two models utilizing PFGE to find the products of homologous, but unequal, crossing-over (triplication) or looping-out (circular DNA) (Fig. 5) and to examine whether

markers flanking the  $p$  locus recombine during the reversion process remain to be done, as does an analysis of the reversion frequency and DNA structure of genetic compounds of various mutant  $p$  alleles with  $p^{un}$ , especially  $p^{un}/p^{6H}$  (duplication/deletion).

**Human Homologue of the  $p$  Locus.** Recently, we have shown that the human homologue of the mouse  $p$  locus is *D15S12*, located on chromosome 15 at q11-q13, a region associated with Prader-Willi syndrome and Angelman syndrome and characterized by profound imprinting effects, genetic instability, and high recombination frequency (2, 5, 23). Although there are imprinting effects localized to mouse chromosome 7 (24-26), no dramatic imprinting effects are reported for the  $p$  locus (6). However, these two syntenic regions may share sequences favoring recombination or genetic instability. Interestingly, duplications involving *D15S12* may have occurred in as many as 6% of Prader-Willi patients (27).

We are grateful to Dr. H. Glenn Wolfe and Dr. Roger Melvold for their communication of unpublished data and we dedicate this paper to them in honor of their original insights into the nature of the  $p^{un}$  mutation. We thank Dr. Eva M. Eicher for generously providing us with mouse strains. We thank Dr. Kenneth Tartof and Dr. Randy Strich for helpful comments on the manuscript. This work was supported by National Institutes of Health Grants GM43840, GM22167, CA06927, and RR05539; by an appropriation from the Commonwealth of Pennsylvania; and by the Pew Charitable Trust. Y.N. is recipient of a Uehara Memorial Fellowship. D.D.-P. was supported by National Institutes of Health Postdoctoral Training Grant CA-09035.

- Wolfe, H. G. (1963) in *Proc. XIth Int. Congr. Genet.* 11, 251.
- Gardner, J. M., Nakatsu, Y., Gondo, Y., Lee, S., Lyon, M. F., King, R. A. & Brilliant, M. H. (1992) *Science* 257, 1121-1124.
- Silvers, W. K. (1979) in *The Coat Colors of Mice* (Springer, New York), pp. 90-101.
- Green, M. C. (1989) in *Genetic Variants and Strains of the Laboratory Mouse*, eds. Lyon, M. F. & Searle, A. G. (Oxford Univ. Press, Oxford), pp. 12-403.
- Brilliant, M. H. (1992) *Mamm. Genome* 3, 187-191.
- Lyon, M. F., King, T. R., Gondo, Y., Gardner, J. M., Nakatsu, Y., Eicher, E. M. & Brilliant, M. H. (1992) *Proc. Natl. Acad. Sci. USA* 89, 6968-6972.
- Melvold, R. W. (1971) *Mutation Res.* 12, 171-174.
- Brilliant, M. H., Gondo, Y. & Eicher, E. M. (1991) *Science* 252, 566-569.
- Phillips, R. J. S. (1977) *Mouse News Lett.* 56, 38.
- Benton, W. D. & Davis, R. W. (1977) *Science* 196, 180-182.
- Schwartz, D. C. & Cantor, C. R. (1984) *Cell* 37, 67-75.
- Dretzen, G., Bellard, M., Sassone-Corsi, P. & Chambon, P. (1981) *Anal. Biochem.* 112, 295-298.
- Sanger, F., Niklen, S. & Coulson, A. R. (1977) *Proc. Natl. Acad. Sci. USA* 74, 5463-5467.
- Weiber, H., Konig, M. & Gruss, P. (1983) *Science* 219, 626-631.
- Marvo, S. L., King, S. R. & Jaskunas, S. R. (1977) *Proc. Natl. Acad. Sci. USA* 80, 2452-2456.
- Tartof, K. D. (1988) *Genetics* 120, 1-6.
- Kelly, R., Bulfield, G., Collick, A., Gibbs, M. & Jeffreys, A. J. (1989) *Genomics* 5, 844-856.
- Jeffreys, A. J., Royle, N. J., Wilson, V. & Wong, Z. (1988) *Nature (London)* 332, 278-281.
- Sturtevant, A. H. (1925) *Genetics* 10, 117-147.
- Matsuoka, M., Yoshida, K., Maeda, T., Usuda, S. & Sakano, H. (1990) *Cell* 62, 135-142.
- Matsuoka, M., Nagawa, F., Kingsbury, L. & Sakano, H. (1992) *Science* 257, 408-410.
- Melvold, R. W. (1972) *Mouse News Lett.* 46, 32.
- Nakatsu, Y., Gondo, Y. & Brilliant, M. H. (1992) *Mamm. Genome* 2, 69-71.
- Searle, A. G. & Beechey, C. V. (1990) *Genet. Res.* 56, 237-244.
- Bartolomei, M. S., Zemel, S. & Tilghman, S. M. (1991) *Nature (London)* 351, 153-155.
- Fergusson-Smith, A. C., Cattanch, B. M., Barton, S. C., Beechey, C. V. & Surani, M. A. (1991) *Nature (London)* 351, 667-670.
- Hamabe, J., Fukushima, Y., Harada, N., Abe, K., Matsuo, N., Nagai, T., Yoshioka, A., Tonoki, H., Tsukino, R. & Niikawa, N. (1991) *Am. J. Med. Genet.* 41, 54-63.